Flutter Design Charts for Biaxially Loaded Isotropic Panels

CHARLES P. SHORE*
NASA Langley Research Center, Hampton, Va.

Until recently, correlation between theory and experiment for flutter of panels stressed to the verge of buckling has not been achieved because of the theoretical prediction of anomalous zero dynamic pressure flutter points. However, a recent linear flutter analysis (NASA TN D-4990) which includes hysteretic structural damping on the bending terms of the flutter equation eliminates the anomalous zero dynamic pressure flutter points and yields good agreement. Thus, it appears that empirical flutter envelopes now used in design, which in many instances are extremely unconservative, can be replaced by design procedures with a more rigorous analytical basis. Toward this end, this paper develops and presents design charts for biaxially loaded isotropic panels on the verge of buckling for typical values of structural damping. Use of these charts permits conservative panel design for wide ranges of panel length-width ratio, in-plane stress ratio, and edge rotational restraint.

Nomenclature

A = $(a/b)^2[k_x - 2]$
a = panel length
b = panel width
c = freestream speed of sound
D = flexural stiffness of isotropic panel
D_1 = $D_x/(1 - \mu_x\mu_y)$
D_2 = $D_y/(1 - \mu_x\mu_y)$
D_{12} = $D_{xy} + \mu_y D_1$
D_x, D_y = flexural stiffness of orthotropic panel in x and y direction, respectively
D_{xy} = twisting stiffness of orthotropic panel
g = structural damping coefficient
i = $(-1)^{1/2}$
k_x = $N_x b^2/\pi^2 D$
M = Mach number
N_x, N_y = in-plane loading in x and y direction, respectively; positive in compression
q = dynamic pressure
q_x, q_y = rotational restraint coefficient on boundary $x = \pm(a/2)$ and $y = \pm(b/2)$, respectively; $a\theta_x/D_1$, $b\theta_y/D_2$
t = time
w = latera' deflection of panel
x, y = Cartesian coordinates of panel
β = Compressibility factor $(M^2 - 1)^{1/2}$
γ = panel mass/unit area
ρ = freestream air density
μ_x, μ_y = Poisson's ratio in x direction and y direction, respectively
θ_x, θ_y = rotational spring constant on boundary $x = \pm(a/2)$ and $y = \pm(b/2)$, respectively

Introduction

RECENT panel flutter investigations[1-3] have shown that theory that adequately accounts for panel edge conditions is in reasonable agreement with flutter results obtained for isotropic and orthotropic panels subjected to moderate levels of in-plane stress. However, at stress levels sufficient to cause buckling, theory indicates that the flutter boundary is extremely sensitive to variations in panel length-width ratio, in-plane stress ratio, and edge condition. In fact, the use of theory that neglects damping results in the prediction of the physically unreasonable value of zero dynamic pressure required for flutter whenever the in-plane load causes the natural frequencies to coalesce for no airflow. Experimental results do not exhibit this anomalous behavior but indicate the flutter q to be a minimum for stressed panels at or near the transition point, represented by the intersection of the unbuckled panel boundary with the buckled panel boundary. Thus, conventional theory is often wholly inadequate for the critical design region and reliance has been placed on experimentally determined flutter envelopes[4,5] for design purposes. Such envelopes are dependent upon a number of parameters, many of which are not investigated in any particular study, and the envelopes are subject to revision as additional experimental data reveal new parameter combinations that lead to more critical flutter conditions. Because reliance on the envelopes involves uncertainties, expensive test programs are often required to insure that flight hardware have adequate stiffness to prevent flutter.

Results from a linear flutter analysis presented in Ref. 6 indicate that proper inclusion of hysteretic structural damping eliminates the anomalous zero dynamic pressure flutter points and yields good agreement with experiment. Thus, it appears that the empirical flutter envelopes can now be replaced by design procedures with a more rigorous analytical basis. Toward this end, the present paper presents design charts developed from the analysis of Ref. 6 for biaxially loaded isotropic panels on the verge of buckling for typical values of structural damping. Use of these charts permits conservative panel designs for wide ranges of panel length-width ratio, in-plane stress ratio, and edge rotational restraint.

Flutter Equation

The flutter analysis presented in Ref. 6 is reviewed in this section. In the analysis, a flat rectangular orthotropic panel of length a and width b is assumed exposed to supersonic flow over one surface; the panel is subjected to uniform in-plane force intensities N_x and N_y which are positive in compression. The panel configuration, loading condition, and coordinate system are shown on Fig. 1. The panel edges are assumed to be elastically restrained from rotations by restoring moments that are of equal magnitude on opposite edges of the panel and are proportional to the edge angle of rotation. The lateral deflection w at all edges is assumed to be zero. Unequal edge rotations and out-of-plane edge deflections have been neglected to simplify the problem.

The small-deflection equilibrium equation for motion of an orthotropic panel in the presence of in-plane compressive loads and supersonic flow with structural damping included

Presented at the AIAA Structural Dynamics & Aeroelasticity Conference, New Orleans, La., April 16 and 17, 1969 (no paper number; published in bound volume of conference papers); submitted May 14, 1969; revision received November 13, 1969.

* Aerospace Engineer. Member AIAA.

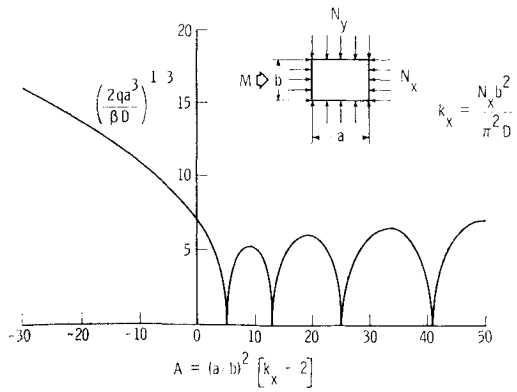

Fig. 1 Classical theory flutter boundary for simply supported panels.

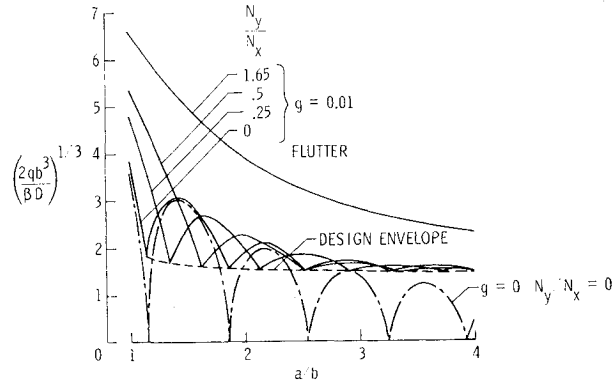

Fig. 3 Transition point flutter boundaries for clamped isotropic panels.

may be written in the following form.[7]

$$(1 + ig)(D_1\partial^4w/\partial x^4 + 2D_{12}\partial^4w/\partial x^2\partial y^2 + D_2\partial^4w/\partial y^4) + N_x\partial^2w/\partial x^2 + N_y\partial^2w/\partial y^2 + \gamma\partial^2w/\partial t^2 + 2q/\beta\partial w/\partial x + pc\partial w/\partial t = 0 \quad (1)$$

Hysteretic structural damping is introduced in Eq. (1) by the concept of complex bending stiffnesses through the factor $(1 + ig)$. The last two terms in Eq. (1) are the aerodynamic lateral loading and the aerodynamic damping terms given by two-dimensional quasi-steady aerodynamic theory. For finite rotational restraint and nondeflecting supports, the boundary conditions are as follows[7]:

$$\begin{aligned} D_1\partial^2w/\partial x^2 - \theta_x\partial w/\partial x &= 0 \text{ and } w = 0 \text{ at } x = -a/2 \\ D_1\partial^2w/\partial x^2 + \theta_x\partial w/\partial x &= 0 \text{ and } w = 0 \text{ at } x = a/2 \\ D_2\partial^2w/\partial y^2 - \theta_y\partial w/\partial y &= 0 \text{ and } w = 0 \text{ at } y = -b/2 \\ D_2\partial^2w/\partial y^2 + \theta_y\partial w/\partial y &= 0 \text{ and } w = 0 \text{ at } y = b/2 \end{aligned} \quad (2)$$

In Ref. 6, a solution to Eq. (1) with boundary conditions given by Eqs. (2) was obtained by application of the Galerkin technique. Sufficient terms (as many as 40) were used in the lateral deflection w to insure convergence of all numerical results.

Characteristics of Solutions to Flutter Equation for Stressed Panels

Flutter boundaries obtained from classical flutter theory[1] are strongly dependent on such parameters as panel length-width ratio a/b, inplane load N_x, and panel boundary conditions. Figure 1 shows such a universal boundary for isotropic panels with simply supported edges. The familiar flutter parameter $(2qa^3/\beta D)^{1/3}$ is shown as a function of A. The parameter A is a combination of the panel length-width ratio a/b and the streamwise in-plane load coefficient k_x, where $k_x = 4$ corresponds to the buckling load for a long simply supported plate subjected to axial compression. It can be seen that at applied loads corresponding to $k_x > 2$, A is positive and large values of a/b correspond to values of the abscissa far to the right. Thus, at certain values of a/b, zero dynamic pressure is predicted for flutter. It should be noted that the flutter boundary is independent of N_y; however, N_y influences the panel buckling point. Thus, N_y influences the location of the transition point.

Inclusion of aerodynamic and structural damping in the flutter theory can remove the zero q flutter points. For example, Fig. 2 shows experimental and theoretical values of the flutter parameter, written in terms of the panel width, as a function of the percent of streamwise buckling load for a rotationally restrained panel with $a/b = 3.3$ and $N_y/N_x = 1$. The circular symbols in Fig. 2 are experimental flutter points obtained at Mach 3 and are taken from Ref. 8. The open symbols are flutter start points with the panel in an unbuckled condition and the solid points are flutter stop points when the panel is buckled. The minimum value of the flutter parameter occurs at the transition point, the intersection of the unbuckled panel boundary and the buckled panel boundary.

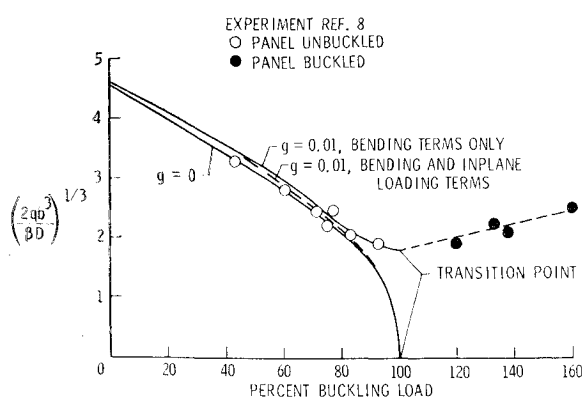

Fig. 2 Comparison of theory and experiment for an isotropic rotationally restrained panel; $a/b = 3.3$, $N_y/N_x = 1$, $q_{xcr} = 40$, and $q_{ycr} = 12$.

The three theoretical curves of Fig. 2 are based on values of rotational restraint coefficients determined from vibration surveys made prior to the flutter tests. A flutter boundary based on classical theory is shown by the lower solid curve. The dashed curve is a flutter boundary obtained with both aerodynamic and structural damping included in the theory and with structural damping incorporated on the in-plane loading terms as well as the bending terms of Eq. (1). This result is shown for completeness because it has been widely used in flutter calculations[9-14]; it is in good agreement with the experimental data at low levels of in-plane stress but predicts zero q flutter at the transition point. The upper solid curve obtained from Eq. (1) with structural damping on only the bending terms, follows the trend of the experimental data and eliminates the anomaly at the transition point. Beyond the transition point where small deflection theory is not adequate, the boundary was faired through the experimental data points. For a more complete discussion of the problems encountered by including structural damping on the in-plane loading terms of the flutter equation, see Refs. 6 and 15.

Because the new calculation agrees well with experimental data at the transition point, conservative design curves based on transition point flutter can be established. The details of constructing these curves are given in the next section.

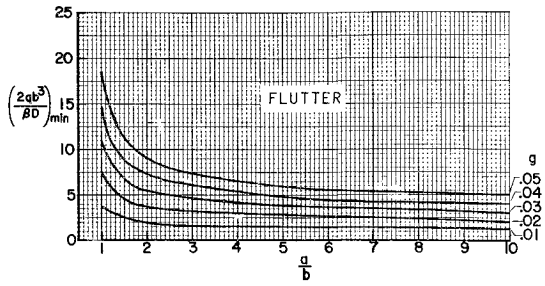

Fig. 4 Flutter design chart for simply supported isotropic panels; $N_y/N_x < 0.5$.

Development of Flutter Design Curves

The procedure for establishing a design curve consisted of calculating transition point values of the flutter parameter for various combinations of a/b, N_y/N_x, edge rotational restraint, and structural damping. A series of such curves is shown in Fig. 3 for panels with clamped edges. The transition point value of the flutter parameter, in terms of the panel width, is shown as a function of a/b. Curves are shown for N_y/N_x = 0, 0.25, 0.5, and 1.65 with $g = 0.01$ and for $N_y/N_x = 0$ with $g = 0$. The curve for $N_y/N_x = 0$ and zero damping (dash-dot curve) was obtained from classical theory and illustrates the extreme sensitivity of the transition point value of the flutter parameter to variations in a/b when damping is neglected. With damping included in the calculations the zero q flutter points no longer appear, but scallops in the flutter boundary still occur especially at the lower values of a/b. As a/b increases for the values of N_y/N_x shown, the scallops in the flutter parameter become less severe, and beyond $a/b = 3$ practically vanish. As N_y/N_x increases, the position of the first minimum moves to the right until at a value of 1.65 it occurs at $a/b = \infty$ and the variation in the flutter parameter becomes monotonic with a/b. For values of N_y/N_x greater than this limiting value, the transition point is removed from the region of the zero q flutter points. For this condition classical theory gives adequate flutter predictions and should be used for design purposes. The limiting value of N_y/N_x is a function of the boundary conditions on edges $y = \pm b/2$ and varies from 0.5 for simply supported edges to 1.65 for fully clamped edges. Since, in practice, it is difficult to know either the stress ratio N_y/N_x or the effective a/b with certainty, it is reasonable to assume that the most critical combinations will occur; thus, the dashed envelope curve through the minimum points is used to establish design charts. This is analogous to using a buckling coefficient for flat plates, which ignors the scallops in the theoretical curve. Thus, in the region of a/b slightly greater than 1 to $a/b = 3$, design charts based on the lower envelope could be moderately conservative for a specific panel; however, for design, the inability to determine N_y/N_x with sufficient certainty precludes reliance on the extra margin.

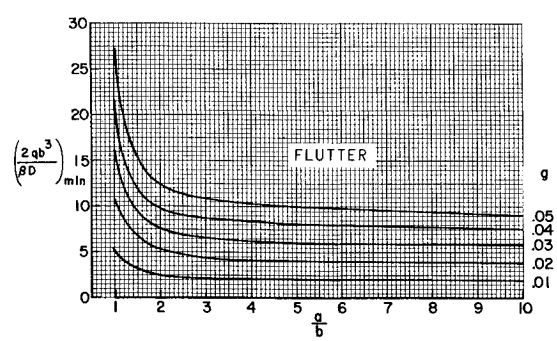

Fig. 5 Flutter design chart for isotropic panels with edge supports of $q_y = 10$ and $q_x = a/b\ q_y$; $N_y/N_x < 1.36$.

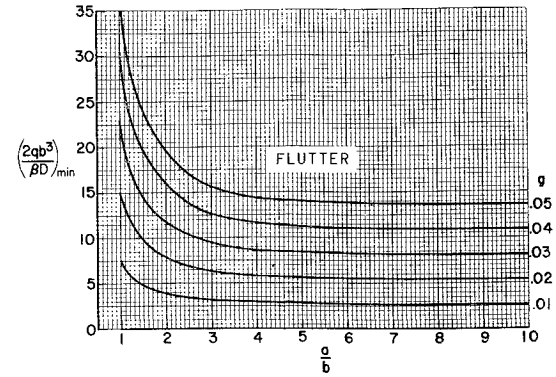

Fig. 6 Flutter design chart for clamped isotropic panels; $N_y/N_x < 1.65$.

Design Charts

Figures 4, 5, and 6 show design curves in terms of $(2qb^3/\beta D)_{min}$ as a function of a/b for values of g from 0.01 to 0.05 and for boundary conditions of simple support, a nondimensional elastic restraint coefficient $q_y = 10$ with $q_x = (a/b)q_y$, and clamped. These curves were obtained by the procedure outlined for Fig. 3 for the values of N_y/N_x which gave the lowest values of the flutter parameter.

Experimental data obtained from tests of panels which can be considered as clamped are compared with the design curves in Fig. 7. The circular symbols are minimum flutter points for single bay panels with an estimated value of $g = 0.01$. Details of the experimental investigations are presented in Refs. 4, 8, and 16–18. The square symbols are minimum flutter points for multibay panels taken from Refs. 5, 19, and 20 and some unpublished data collected by R. W. Hess in the Langley Unitary Plan Wind Tunnel. Damping coefficients were measured by Hess and ranged from $g = 0.02$ to 0.05. Open symbols represent panels with $N_y/N_x \approx 1$ and the solid symbols represent panels with $N_y/N_x \approx 0$.

Several of the data points on Fig. 7 at low values of a/b fall well above the design curves. As shown in Fig. 3, at the smaller values of a/b the stress ratio can have a significant effect on the transition point. If this effect is taken into account, the classical flutter solution without damping is conservative but reasonably accurate. The dashed curves in Fig. 7 are transition point values taken directly from Ref. 1

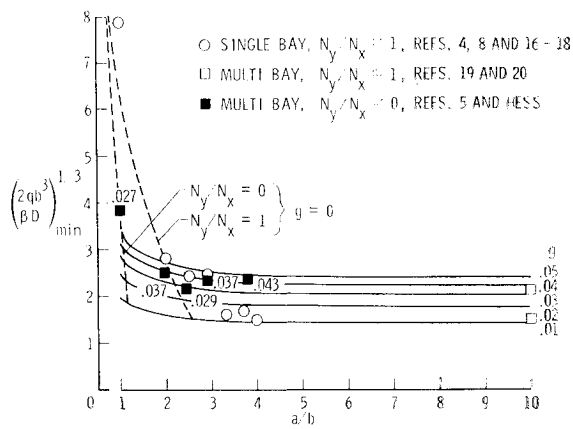

Fig. 7 Comparison of test data with design curves for clamped panels; $N_y/N_x < 1.65$. (Numbers adjacent to test points denote measured value of damping coefficient.)

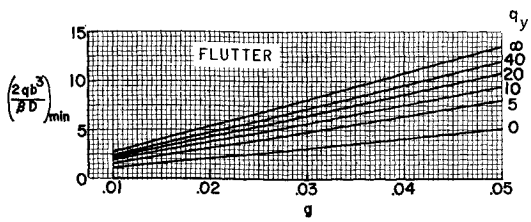

Fig. 8 Flutter design chart for panels with $a/b > 4$.

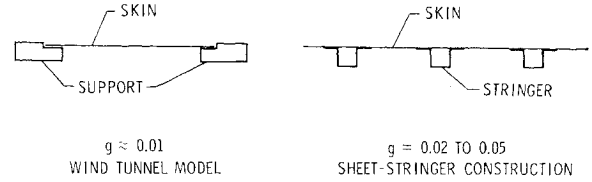

Fig. 9 Values of structural damping coefficient for typical panel constructions.

and are seen to give a conservative prediction for the rapid decrease in the transition point value of the flutter parameter exhibited by the experimental panels as a/b increases. The fact that the data point of $a/b = 1$ for $N_y/N_x \approx 1$ does not agree very well with the theory can be attributed in part to inexact knowledge of the value of a/b and N_y/N_x present in the experimental investigation of Ref. 18. It should be emphasized at this point for small values of a/b the results of Ref. 1 should be utilized for design purposes until the predicted value of the flutter parameter falls below those predicted by the present design charts. In the region of $a/b > 2$, the design curves are in good agreement with the data and give conservative flutter predictions.

The curves in Figs. 3–6 indicate that for long panels flutter becomes independent of the panel length and N_y/N_x. Thus, one set of curves for a range of damping coefficients and rotational restraint coefficients is sufficient for design of long panels. This is shown in Fig. 8 where the minimum value of the flutter parameter is plotted as a function of g with lateral edge rotational restraint from $q_y = 0$ (simple supports) to $q_y = \infty$ (clamped). The curves in Fig. 8 indicate the beneficial effects of increasing edge rotational restraint and structural damping and are reasonably accurate for all panels with a/b greater than 4.

The linear analysis used to develop the design charts cannot account for the nonlinear effects of large panel deflections, lateral edge deflections, and differential pressure. Shear edge loadings were neglected to simplify the analysis; however, for large values of a/b the flutter parameter is insensitive to biaxial stress combinations and will probably remain so with the inclusion of shear edge loadings. Most of the previous factors were present to some extent in the experimental data shown in Fig. 7 and do not appear to greatly influence the good correlation with theory shown therein. Variation of the flutter parameter with edge rotational restraint is not large, such that interpolation to obtain design values of the flutter parameter when opposite edges of the panel do not have equal rotational restraint, is reasonably accurate.

These factors indicate that the design charts can be utilized with some degree of confidence for typical skin-stringer panel designs over a wide range of stress and edge support conditions whenever the panel supports have sufficient stiffness to cause buckling node lines to occur along the supports.

In order to use the design charts, a value of the structural damping coefficient g must be reasonably well known. There has been a large amount of research on the mechanisms, measurement, and prediction of structural damping in recent years. Lazan[21] summarizes the state-of-the-art for the field of structural damping and gives the best available techniques for predicting structural damping coefficients. Values of g from 0.001 to 0.01 are reported for metallic materials whereas values up to 0.2 are reported for fabricated structures. However, adequate flutter predictions require that g be more closely evaluated. Figure 9 shows the types of panel construction employed in obtaining the experimental data shown in Fig. 7. The first type represents wind-tunnel research models and consists of a single bay with rather massive supports. No damping coefficients were measured but a value of 0.01 appears to correlate the experimental flutter data with the theoretical results shown in Fig. 7. The second type consists of multibay panels supported by ribs and stringers and is fairly representative of actual aerospace construction. The damping coefficients measured by Hess on panels representative of aerospace construction indicated considerable variation between panels and varied for a given panel as the amount of in-plane stress varied. The values of damping shown in Fig. 7 were obtained at stresses up to approximately 50% of the buckling stress. A value of $g = 0.03$ was a typical measured value for these test panels. However, Ref. 21 points out that factors such as material, thickness, stress level, type of loading, temperature, and panel construction details greatly affect the damping coefficient and that care must be exercised in arriving at a reasonable estimate of g. Initial panel design should be based on values of g obtained utilizing the techniques outlined by Lazan.[21] Additionally, to insure adequate flutter margins it would be prudent to construct representative panels and measure actual levels of g. However, in the absence of other data $g = 0.03$ appears to correlate flutter results for panels of typical aircraft construction whereas $g = 0.01$ appears to be a practical design lower limit.

Concluding Remarks

The anomalous zero q flutter points which have been predicted by classical theory for panels on the verge of buckling have been eliminated by inclusion of linear, hysteretic, frequently independent, structural damping on the bending terms of the flutter equation. This procedure reduces the sensitivity of the flutter parameter to variations in length-width ratio a/b, stress ratio N_y/N_x, and boundary conditions, and gives good agreement with experiment at the transition point which is usually the most critical flutter point. Results from the theory enabled construction of flutter design charts as a function of structural damping. Curves of flutter q vs a/b with different damping coefficients are presented for three values of edge rotational restraint. Use of the charts allows rapid prediction of the minimum flutter q for wide ranges of a/b, N_y/N_x, and edge rotational restraint for values of structural damping $g = 0.01$ to 0.05. A value of $g = 0.03$ might be considered a reasonable value for panels typical of present aircraft construction practice whereas $g = 0.01$ appears to be a practical design lower limit.

References

[1] Erickson, L. L., "Supersonic Flutter of Flat Rectangular Orthotropic Panels Elastically Restrained Against Edge Rotation," TN D-3500, 1966, NASA.

[2] Shideler, J. L., Dixon, S. C., and Shore, C. P., "Flutter at Mach 3 of Thermally Stressed Panels and Comparison with Theory for Panels With Edge Rotational Restraint," TN D-3498, 1966, NASA.

[3] Bohon, H. L. and Anderson, M. S., "Role of Boundary Conditions of Flutter of Orthotropic Panels," *AIAA Journal*, Vol. 4, No. 7, July 1966, pp. 1244–1248.

[4] Kordes, E. E., Touvila, W. J., and Guy, L. D., "Flutter Research on Skin Panels," TN D-451, 1960, NASA.

[5] Hess, R. W. and Gibson, F. W., "Experimental Investigation of the Effects of Compressive Stress on the Flutter of a

Curved Panel and a Flat Panel at Supersonic Mach Numbers," TN D-1386, 1962, NASA.

[6] Shore, C. P., "Effects of Structural Damping on Flutter of Stressed Panels," TN D-4990, 1968, NASA.

[7] Libove, C. and Batdorf, S. B., "A General Small Deflection Theory for Flat Sandwich Plates," Rept. 899, 1948, NACA.

[8] Shore, C. P., "Experimental Investigation of Flutter at Mach 3 of Rotationally Restrained Panels and Comparison with Theory," TN D-5508, 1969, NASA.

[9] Kobett, D. R. and Zeydel, E. F. E., "Research on Panel Flutter," TN D-2227, 1963, NASA.

[10] Nelson, H. C. and Cunningham, H. J., "Theoretical Investigation of Flutter of Two-Dimensional Flat Panels with One Surface Exposed to Supersonic Potential Flow," Rept. 1280, 1956, NACA.

[11] Dowell, E. H. and Voss, H. M., "Theoretical and Experimental Panel Flutter Studies in the Mach Number Range 1.0 to 5.0," *AIAA Journal*, Vol. 3, No. 12, Dec. 1965, pp. 2292–2304.

[12] Johns, D. J. and Parks, P. C., "Effect of Structural Damping on Panel Flutter," *Aircraft Engineering*, Vol. XXXII, No. 380, Oct. 1960, pp. 304–308.

[13] Cunningham, H. J., "Flutter Analysis of Flat Rectangular Panels Based on Three-Dimensional Supersonic Unsteady Potential Flow," TR R-256, 1967, NASA.

[14] Dixon, S. C., "Comparison of Panel Flutter Results from Approximate Aerodynamic Theory with Results from Exact Inviscid Theory and Experiment," TN D-3649, 1966, NASA.

[15] Ellen, C. H., "Influence of Structural Damping on Panel Flutter," *AIAA Journal*, Vol. 6, No. 11, Nov. 1968, pp. 2169–2174.

[16] Dixon, S. C. and Shore, C. P., "Effects of Differential Pressure, Thermal Stress, and Buckling on Flutter of Flat Panels with Length-Width Ratio of 2," TN D-2047, 1963, NASA.

[17] Dixon, S. C., "Application of Transtability Concept to Flutter of Finite Panels and Experimental Results," TN D-1948, 1963, NASA.

[18] Dixon, S. C., "Experimental Investigation at Mach Number 3.0 of Effects of Thermal Stress and Buckling on Flutter Characteristics of Flat Single-Bay Panels of Length-Width Ratio 0.96," TN D-1485, 1962, NASA.

[19] Dixon, S. C., Griffith, G. E., and Bohon, H. L., "Experimental Investigation at Mach Number 3.0 of the Effects of Thermal Stress and Buckling on the Flutter of Four-Bay Aluminum Alloy Panels with Length-Width Ratios of 10," TN D-921, 1961, NASA.

[20] Guy, L. D. and Bohon, H. L., "Flutter of Aerodynamically Heated Aluminum-Alloy and Stainless Steel Panels with Length-Width Ratio of 10 at Mach Number of 3.0," TN D-1353, 1962, NASA.

[21] Lazan, B. J., *Damping of Materials and Members in Structural Mechanics*, 1st ed., Vol. 1, Pergamon Press, New York, 1968.